INTERNATIONAL JOURNAL OF MECHANICS
DOI: 10.46300/9104.2023.17.7 Volume 17, 2023

Experimental models of the lateritic minerals drying kinetics at high temperatures

Torres Tamayo Enrique[1], Zalazar Carlos[2], Morales José[4], Carrión Daniel[3], Iza Edison[4], Reinoso Edgar[4], Góngora Ever[2]
[1]Cotopaxi Technical University, Latacunga City, 050101, ECUADOR
[2]Metallurgical Mining Higher Institute, Moa City, 83310, CUBA
[3]San Francisco University, Quito City, 170102. ECUADOR
[4]Cyfoil, Constructions and Oil Facilities, 050101, ECUADOR

Received: February 24, 2023. Revised: March 12, 2023. Accepted: April 23, 2023. Published: May 12, 2023.

Abstract — **In the present investigation, a study of the drying kinetics of lateritic mineral samples is carried out and the adjustment of the theoretical models exposed in the specialized literature with the data obtained during the experimentation is evaluated. The variation of humidity, drying speed, and drying time for temperatures between 100 ºC and 500ºC were analyzed. In addition, for each of the temperatures studied, the adjustment constants of the theoretical models were determined. From the comparison of the theoretical models, it is established that the Modified Page model is more adjusted to the behavior obtained from the lateritic mineral. From the analysis of the drying curves, it is concluded that the lateritic mineral has a non-hygroscopic behavior.**

Keywords —**Lateritic mineral, drying, drying kinetics.**

I. INTRODUCTION

The nickel reserves are found as nickel oxide in lateritic ores. Currently, more than 51% of nickel production comes from the processing of laterite, [1], which is mined from open pit mines with moisture concentrations of approximately 45%.

These minerals are usually subjected to a drying process at high temperatures in direct contact rotary dryers (between 750 ºC and 850 ºC at the inlet of the dryer and 90 ºC and 100 ºC at the outlet). However, there is little information available in the literature on the drying kinetics of this material, [2], which makes it difficult to characterize and model this process at high temperatures in rotary dryers.

In [3], [2], [4], the authors analyze the drying kinetics of lateritic mineral samples for temperature ranges between 44 ºC and 228 ºC. More recent studies, [5], study the kinetics of drying using a microwave oven as a drying alternative to reduce the emission of The duration of the constant speed drying period depends on the heat and mass transfer coefficients, the area exposed to the drying medium, the geometry of the sample and the difference in temperature and humidity between the drying When the constant drying stage is finished, the decreasing rate period (C-D) begins; where the moisture linked to the material evaporates and the internal and external conditions prevail simultaneously. The temperature of the material exceeds that of the wet bulb due to the decrease in the drying speed, which breaks the thermal equilibrium that keeps the temperature stable, and a considerable part of the heat is used in heating the solid, [10], medium current and the surface wet from the solid, [9], polluting gases into the atmosphere. Other model development for lateritic mineral pneumatic conveying in dilute and dense phases in horizontal and vertical pipes was developed taking into consideration the variety of physical and aerodynamic characteristics of the materials to transport, [6].

Although these studies present interesting and valuable results for researchers and technicians of the mining and metallurgical industries, they are still insufficient to characterize the behavior of moisture migration inside a direct contact dryer that operates at high temperatures. Therefore, the objective of the present work is to evaluate various kinetic drying models in lateritic mineral samples for temperatures between 100 ºC and 500 ºC.

In the specialized literature, several theories explain the moisture transport in porous media, for which various general models have been developed. The simplest consideration is that there is only one mechanism responsible for moisture migration. However, other studies identify more than one mechanism during the different drying stages, [7].

According to [7], the drying in porous materials can occur through the following mechanisms:

- Liquid diffusion: due to moisture concentration gradients.
- Steam diffusion: due to partial pressure gradients of steam.
- Liquid movement: due to capillary forces.
- Liquid or vapor flow: due to differences in the pressure that exists inside the pores and the drying agent.
- Effusion: occurs when the mean free path of the vapor molecules is of the order of the diameter of the pores.
- Liquid movement: due to gravity.
- Surface diffusion: due to the moisture concentration gradients and the partial pressure of the vapor that is generated on the drying surface.

According to [8], the drying process is divided into the following stages (Figure 1). The first stage is called heating: comprised from A to B, it has a short duration and in it, the evaporation is not significant due to its intensity or its

quantity. The solid is heated from room temperature to equilibrium between evaporative cooling and the absorption of heat from the gases.

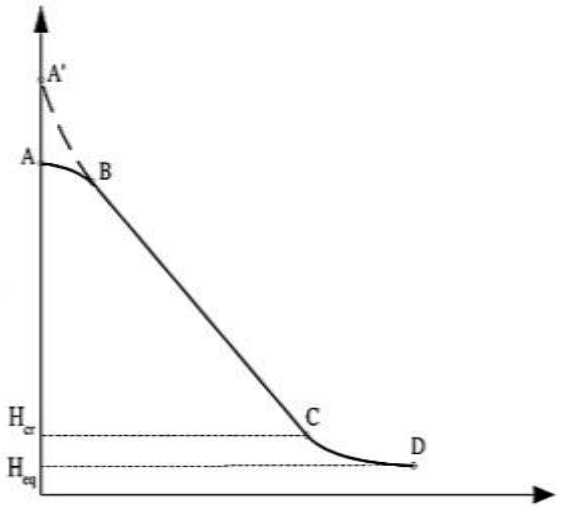

Figure 1. Stages of drying

The most widespread models based on the aforementioned theories are those that consider the simultaneous diffusion of vapor and liquid, those based on the thermodynamics of irreversible processes, and those based on the simultaneous transfer of heat and mass, [11], [12].

In addition, there are experimental models which constitute a useful tool when simplifying the study of drying processes. With these, the drying kinetics are determined in a simple way and with an acceptable degree of precision, [13]. The most widespread experimental theoretical models in the literature are presented in Table 1, [14].

Table 1. Experimental models describing the drying kinetics

Name	**Model**
Newton	$R_H = e^{-k \cdot t}$
Page	$R_H = e^{-k \cdot t^n}$
Henderson and Pabis	$R_H = a \cdot e^{-k \cdot t}$
Logarithmic	$R_H = a \cdot e^{-k \cdot t} + c$
Two terms experimental	$R_H = a \cdot e^{-k \cdot t} + (1 - a) \cdot e^{-k \cdot b \cdot t}$
Wang and Singh	$R_H = 1 + a \cdot t - b \cdot t^2$

Being k, n, c, and b coefficients of adjustment of the models. These models have been used successfully for the mathematical modeling of the drying process in products such as: grains, fertilizers, and wood, [15].

II. METHOD DEVELOPMENT

Characterization of lateritic ores

The lateritic mineral studied is composed of essentially ferrous materials. The chemical composition of this and the percentages by elements are shown in Table 2.

Table 2. Chemical composition of the lateritic mineral

Element	**Ni**	**Fe**	**Co**	**SiO_2**	**MgO**
%	1,18 – 1,24	36,5 – 40,69	0,090 – 0,101	10,05 – 13,0	4,29 – 7,0

The granulometry ranges between 0 and 50 mm, which represents 80.72 % of the total weight of the samples. The mineralogical composition is characterized by the predominance of Goethite which represents 64.58 % to 70.68 % on average, [16].

Experimental facility

The experiments were carried out in the laboratory of the Nickel Industry Research and Development Unit.
The equipment used in the experiments were the following:

- Precision analytical balance;
- Stove;
- Crucibles with their lids;
- Beaker; Pipette;
- Wet bulb and dry bulb thermometer
- Sieve.

Experiment design

In the experimentation, five temperature values were analyzed, ranging from 100ºC to 500ºC. The initial humidity of the samples was 54% based on the dry mass. In each experiment, five replications were carried out and the average among the five was determined according to the scheme shown in Figure 2.

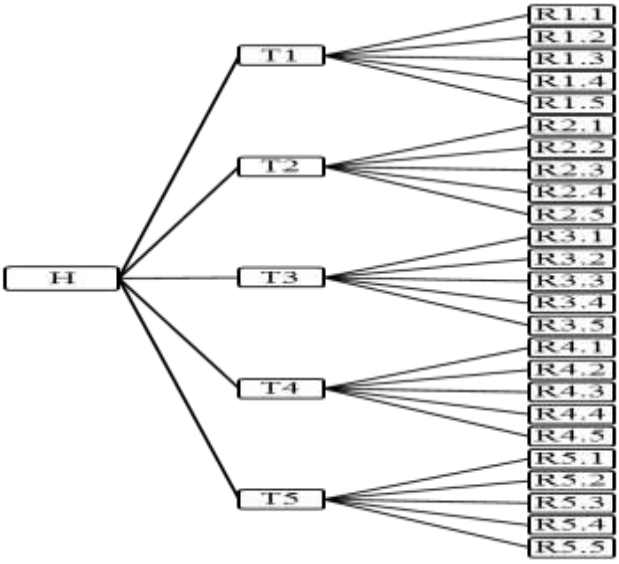

Figure 2. Experimental diagram

H: initial humidity of the sample, %
T1-T5: are the temperatures studied, ºC
Ra.b: are the replicates where ¨a¨ represents the experiment number and ¨b¨ the replicate number of the experiment.

The procedure used in the experimentation

For the experimentation, the procedure described below was applied:
Sampling and sample preparation

- The samples are taken randomly from the dynamic flow at the outlet of the grinder with a maximum granulometry of 30 mm with an approximate weight of 10 to 12 kg. It is then homogenized using the quartering method or the cone and ring method.
- The sample to be analyzed is dried for 24 h at a temperature of 150 ºC to guarantee that the mineral is completely dry.

Experimentation

- From the totally dry sample, 100 g are taken in different previously tared crucibles and 54 g of water are added to them to ensure that all the samples have the same initial humidity, then the initial weights of each of them are taken.
- The crucibles are placed in the oven at the temperature determined according to the experiment that is carried out and for a certain time.
- Once the time has elapsed, the samples are extracted and placed in a desiccator until they cool to room temperature.
- Subsequently, the samples are placed on an analytical balance and the weights are taken at room temperature.
- By weight difference, the humidity corresponding to time is determined, and the procedure is repeated so on until finally obtaining the dynamic equilibrium humidity or humidity values close to 0, 01 g / g.

Method for the evaluation of the results obtained in the experimentation

For the analysis and evaluation of the results obtained from the experimentation, the following expressions that characterize the process were used.

Moisture content: to determine the moisture content present in the sample, equation (1) is used to determine humidity based on dry mass (Hbs).

$$H_{bs} = \frac{m_h}{m_s} = \frac{m_0 - m_s}{m_s} \quad (1)$$

m_h- Mass of water in wet material (g)

m_0- Mass of water in wet material (g)

m_s- Dry mass of solid (g)

The Humidity Ratio (R_h) or humidity ratio is calculated by equation (2).

$$R_h = \frac{H_t - H_e}{H_0 - H_e} \quad (2)$$

R_h- Drying ratio; Dimensionless

H_t- Instant humidity; g/g

H_0- Initial humidity; g/g

However, it is usual to neglect the equilibrium moisture content (He), in this way the expression for the moisture ratio is as follows (3).

$$R_H = \frac{H_t}{H_0} \quad (3)$$

The drying rate or drying speed of the product expressed in terms of the mass of evaporated water per unit of time (g/g·s) is determined by equation (4).

$$R_s = \frac{dH}{dt} = \frac{H_{t+dt} - H_t}{dt} \quad (4)$$

Determination of drying kinetic constant

To determine the drying kinetic constant, it is carried out in a similar way to the methodology developed by the following researchers, [17].

With the data obtained from the experimentation, the adjustment parameters (k, a, c, and n) are determined in correspondence with the existing models (Table 1) where k is the drying kinetic constant. Once the model that best fits the experimental data and the drying constant has been found, the influence of temperature on this process is evaluated from the Arrhenius equation (5).

$$k = b \cdot \exp\left(\frac{-E_a}{R_g \cdot T_g}\right) \quad (5)$$

Where:

E_a- Activation energy (J/mol)

R_g- Universal gas constant (8,3143 J/mol K)

When evaluating the relationship obtained between the natural logarithm of the speed constant and the inverse of the temperature, a linear behavior defined by equation (6) is obtained.

$$\ln(k) = m \cdot \frac{1}{T_g} + b \quad (6)$$

Where m is the slope of the line and it will be equal to the division of the activation energy with the universal gas constant (-Ea/Rg), Tg is the drying temperature (K), and b is the intercept with the vertical axis.

III. RESULTS AND DISCUSSION

With the averages of the five replications carried out for each of the experiments, the behavior shown in Figure 3 was obtained, which shows the effect of temperature on the drying rate of the lateritic mineral, corroborating that as the temperature increases it also increases the drying rate and the drying time is shortened (Figure 3).

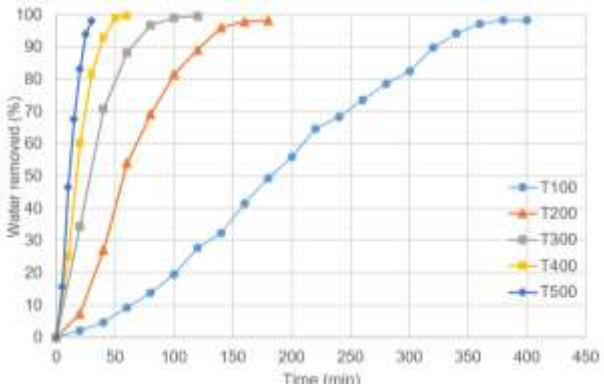

Figure 3. The behavior of the Water removed as a function of the time

It is also observed that the times required to reach a moisture content of approximately 0.01 kg water/kg of the dry mineral were 50, 60, 100, 160, and 380 min for temperatures of 500; 400; 300; 200, and 100 ° C, respectively (Figure 4).

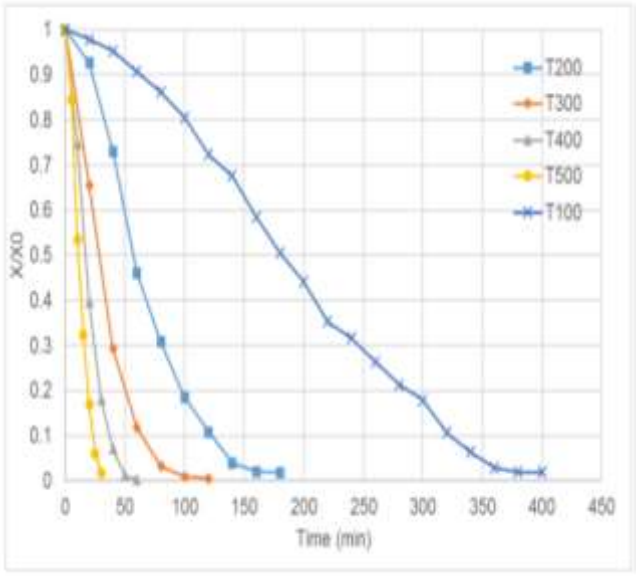

Figure 4. The behavior of the Water removed as a function of the time.

The behaviors obtained with the drying curve show that they have an almost straight section that corresponds to the drying stage at a constant speed and a curved section that corresponds to the drying stage at a decreasing speed. When the straight section is finished and the curve is started, the critical time and critical humidity are read on the graph. It is also observed that the curve has an asymptotic behavior with the abscissa axis (time) and allows the establishment of the equilibrium humidity (Figure 5).

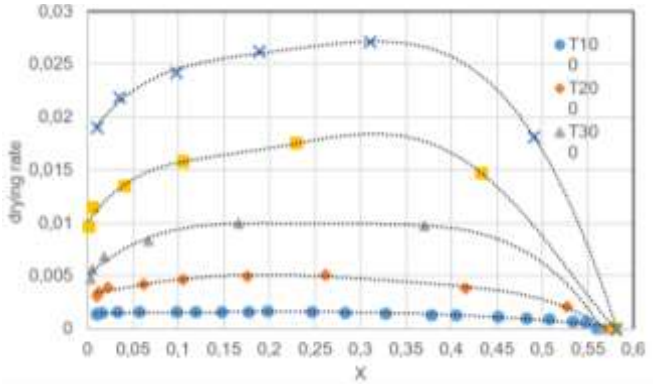

Figure 5. Drying rate as a function of humidity variation.

Figure 6 shows the behavior of the different stages of the lateritic mineral drying process. In the analysis of the drying curves, the characteristics of a porous non-hygroscopic porous solid were exhibited. It was also verified during the drying process of the lateritic mineral that the three phases or periods of drying, heating, constant speed, and decreasing drying intervene.

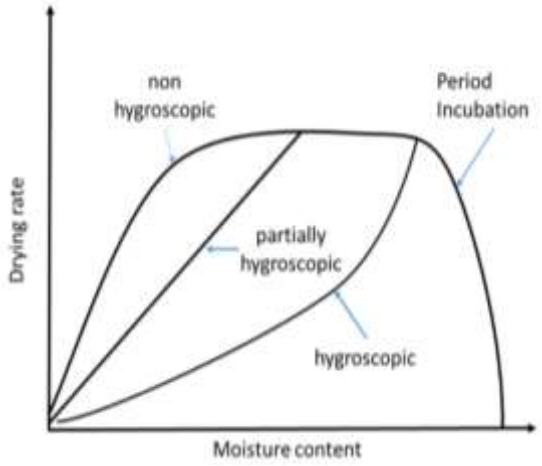

Figure 6. Different stages of the lateritic mineral drying process.

However, when analyzing the behaviors obtained from the drying ratio (Figure 5 and Figure 6) for the tested temperatures, it was determined that the drying periods are not only that of constant speed and period of decreasing speed. As can be seen, the three drying periods are involved. Relatively short heating period, a period of a constant rate of drying, and finally a period of drying at decreasing rate. The stretch that grows corresponds to the heating request (Period I), and the straight stretch with respect to the horizontal (Period II) is the period of constant drying speed and is associated with the elimination of water not bound to the product, in which the water behaves as if the solid were not present.

At the beginning, the surface of the product is very wet, the water removed on the surface is compensated by the flow of water from the interior of the solid. The period of constant velocity continues as long as the evaporated water on the surface can be offset by that found in the interior. The period of decreasing speed (Period III) occurs when the drying speed does not remain constant and begins to decrease.

In addition, it was determined that the behavior of the lateritic mineral is typical of a non-hygroscopic porous solid, according to that shown in Figure 6, where the mechanisms that control the flow of heat for heating the sample are short. These results agree with that obtained by [4].

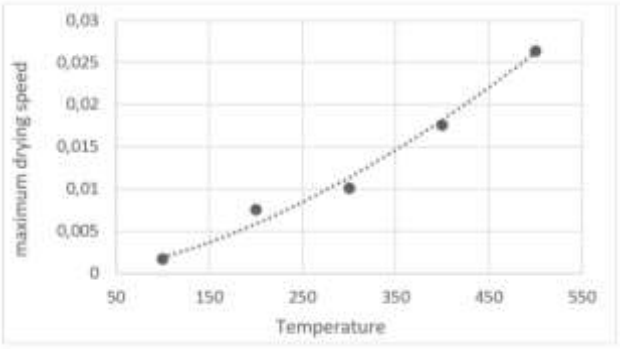

Figure 7- maximum drying speed

Figure 7, shows the maximum values of drying speed as a function of temperature to evaluate how the temperature affects this parameter. As can be seen, the maximum rate of the dryer speed for each of the temperatures corresponds to when the heating period ends. For the temperature of 100ºC,

it corresponds to the constant drying period while for the remaining temperatures, the highest drying rate occurs in the period of decreasing speed.

Drying kinetic constant

To determine the behavior of the variation of humidity, the humidity ratio, and the drying speed of the lateritic mineral sample, the adjustment of the models most used in the specialized literature (Newton; Page; Modified Page; Handerson and Pabis; Logarithmic) to the results obtained in the experimentation.

Table 3. Comparison of the experimental values and the adjusted theoretical models.

Theoretical models	T (ºC)	R_2	RMSE	Model Fit Constants			
				k	n	a	b
Newton	100	0,92	0,0893	0,003918			
	200	0,91	0,1163	0,0158			
	300	0,967	0,0742	0,03175			
	400	0,948	0,0802	0,05109			
	500	0,964	0,0708	0,08128			
Page	100	0,993	0,0254	9,11E-0,5	1,687		
	200	0,994	0,0242	0,000115	1,644		
	300	0,999	0,0054	0,004009	1,571		
	400	0,990	0,0282	0,009193	1,562		
	500	0,995	0,0266	0,02127	1,505		
Modified Page	100	0,993	0,0254	0,004027	1,687		
	200	0,997	0,0209	0,0141	1,943		
	300	0,999	0,0051	0,02984	1,58		
	400	0,994	0,0274	0,04907	1,62		
	500	0,998	0,0139	0,07698	1,622		
Handerson and Pabis	100	0,943	0,0770	0,004387		1,155	
	200	0,919	0,1189	0,01824		1,216	
	300	0,966	0,0875	0,03306		1	
	400	0,952	0,0821	0,05733		1,137	
	500	0,962	0,0797	0,07716		1	
Logarithmic	100	0,997	0,0166	0,000665		4,209	-3,168
	200	0,979	0,0656	0,006089		1,91	-0,8456
	300	0,991	0,0533	0,01977		1,305	-0,2884
	400	0,997	0,0220	0,02063		1,837	-0,8165
	500	0,993	0,0377	0,04912		1,348	0,328

Table 3, shows the results obtained from the comparison of the experimental values and the adjusted theoretical models for the laterite mineral analyzed. According to the results obtained, it was found that any of the analyzed models can be used quite accurately. Considering that the values of the correlation coefficients and the errors of the models are acceptable.

Where:
T- Experimental temperature (ºC)
R2- Correlation coefficient
RMSE- Root mean square error
k, n, a, b- Model fit constants

However, due to its precision and simplicity, the modified Page model was used to determine the kinetic constant of drying, in which values of "k" between 0.004 to 0.07 and values of R2 between 0.9938 and 0.999 were obtained for the temperature ranges between 100 ºC and 500 ºC. Figure 8 and equation (7) show the linear fit of the constant "k".

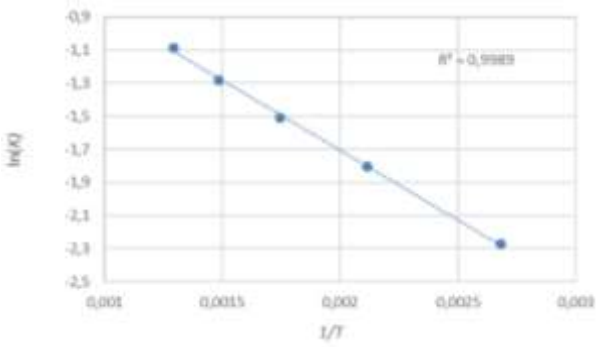

Figure 8. Linear fit of ln(K)

$$ln(k) = -914{,}3 \cdot \frac{1}{T_g} + 0{,}0655 \quad (7)$$

The coefficients of the equation that determine the slope and the intersection of the line are substituted in the Arrhenius equation, obtaining equation (8) that characterizes the kinetic constant of the lateritic mineral as a function of temperature.

$$k = 0{,}0655 \cdot exp\left(\frac{-914{,}3}{T_g}\right) \quad (8)$$

IV. CONCLUSIONS

- The drying kinetics of the lateritic mineral was analyzed for temperature ranges from 100 ºC to 500 ºC using the technique known as thermogravimetry.
- In the analysis of the drying curves, the characteristics of a porous non-hygroscopic porous solid were exhibited. It was also verified during the drying process of the lateritic mineral that the three phases or periods of drying, heating, constant speed, and decreasing drying intervene.
- From the comparison of the experimental data with the theoretical models, it was determined that the one with the best fit is the Modified Page model. With this, values of the constant "k" between 0.004027 and 0.07698 were obtained for the temperature ranges from 100 ºC to 500 ºC.

REFERENCES

[1] Li, J. et al (2018). Selective leaching of valuable metals from laterite nickel ore with ammonium chloride-hydrochloric acid solution. Journal of Cleaner Production, 179 (1), p. 24-30.

[2] Pickles, C. (2003). Drying kinetics of nickeliferous limonitic laterite ores. Journal of Minerals Engineering. 16 (12), p. 1327–1338.

[3] Torres, E. et al (2003). Analysis of the temperature regime influence on lateritic mineral drying. Journal of Minería y Geología. 1 (2), p. 118-123.

[4] Pickles, C. (2005). Microwave drying of nickeliferous limonitic laterite ores. Journal of Canadian Metallurgical Quarterly. 44(3), p. 397-408.

[5] Wei L. et al. (2021). Drying kinetics of a Philippine Nickel Laterite Ore by Microwave Heating. Journal of Mineral processing and extractive metallurgy review. 42(1), p. 01-07.

[6] Torres T. E., et al (2017). Energy consumption and simulation of pneumatic conveying lateritic mineral in dense and fluid phase. International Journal of Mechanics, vol. 11, pp. 12–17. ISSN: 19984448.

[7] Hernández J. and D. Quinto (2005). Drying of Porous Mediums: a Theorical Review of Actual Techniques. Journal of Científica. 9(2): p. 63 - 71.
[8] Carl H. (1980). Handbook of Industrial Drying. Hemisphere, New York: p. 1 – 1279.
[9] Fortes M. and M. Okos (1980). Drying Theories: Their Bases an Limitations as Applied to Food and Grains. Advances in Drying. Journal of Hemisphere Publishig: p. 119 – 154.
[10] Lewis, W.K. (1921) The Rate of Drying of Solid Materials. Journal of Industrial & Engineering Chemistry, 13, p. 427-432. https://doi.org/10.1021/ie50137a021.
[11] Kowalski S. (2001). Thermomechanical Approach to shrinkin and cracking phenomena in drying. Journal of drying technology. 19(5): p. 731-765.
[12] Kowalski S.J. and C.C. Strumillo (1997). Moistur transport, thermodynamics, and boundary conditions in porous materials in presence of mechanical stresses. Journal of chemical Engineering Science. 52(7): p. 1141-1150.
[13] Villalba V. et al (2015). Mathematical and experimental models for drying of biomass. Journal of Ingeniería y Desarrollo. 33(2): p. 301-330.
[14] Mazutti M. et al (2010). Mathematical modeling of thin-layer drying of fermented and non-fermented sugarcane bagasse. Journal of Biomass and Bioenergy. 34 (1): p. 780-786.
[15] Ingle M. et al (2019). Drying Kinetics and Mathematical Modeling of Beetroot. International Journal of Current Microbiology and Applied Sciences. 8 (1): p. 1926-1934.
[16] Rojas A. (2001). Evidences in favour to consider the goethite phaseas the main nickel-bearing mineral in ferruginous lateritic nickel ores. Journal of Minería & Geología. 18 (3-4): p. 21 - 31.
[17] Umaña M. et al. (2019). Modelling of thin layer radiation drying of coconut. Journal of Tecnología en Marcha. 32(1): p. 115-121. https://doi.org/10.18845/tm.v32i7.4269.

Contribution of individual authors to the creation of a scientific article (ghostwriting policy)

-Torres Tamayo Enrique and Carlos Salazar have obtained the model of the lateritic mineral drying kinetics

-Góngora Ever, Morales José, Carrión Daniel, Iza Edison and Reinoso Edgar carried out experiments in section III

Sources of funding for research presented in a scientific article or scientific article itself

No funding was received for conducting this study.

Conflict of Interest

The authors have no conflict of interest to declare.